1 # A non-vesicular Argonaute protein is transmitted from nematode to
2 mouse and is important for parasite survival

3

4 Kyriaki Neophytou[1], Isaac Martínez-Ugalde[2,3#], Thomas Fenton[1,4#], Elaine Robertson[1],
5 Lewis J. Strachan[1,5#], Yvonne Harcus[1], Chanel M. Naar[1,6#], David Wright[1], Daniel R. G.
6 Price[7], Ruby White[1,4#], Michael J. Evans[1,2#,8#], Jose R. Bermúdez-Barrientos[1,9#], Hanchen
7 Li[10], Rick M. Maizels[4], Raffi V. Aroian[10], Alasdair J. Nisbet[7], Cei Abreu-Goodger[2], Amy H.
8 Buck[1, 11, *]

9

10 [1] Institute of Immunology and Infection Research, School of Biological Sciences, The
11 University of Edinburgh, Edinburgh, EH9 3FL, UK

12 [2] Institute of Ecology and Evolution, School of Biological Sciences, The University of
13 Edinburgh, Edinburgh, EH9 3FL, UK

14 [3] Department of Molecular Genetics, Faculty of Medicine, University of Toronto, Toronto,
15 ON M5S 1A8 Canada

16 [4] School of Immunity & Infection, University of Glasgow, Glasgow, G12 8TA, UK

17 [5] Cambridge Institute for Medical Research, University of Cambridge, Cambridge, CB2
18 0XY, UK

19 [6] Leiden University Center for Infectious Diseases, Leiden University Medical Center,
20 Leiden, 2333ZA, Netherlands

21 [7] Department of Vaccines and Diagnostics, Moredun Research Institute, Edinburgh, EH26
22 0PZ, UK

23 [8] Department of Disease Control, Moredun Research Institute, Edinburgh, EH26 0PZ, UK

24 [9] Cancer Research UK Scotland Institute, Switchback Road, Bearsden, Glasgow, G61
25 1BD, UK

26 [10] University of Massachusetts Chan Medical School, Program in Molecular Medicine,
27 Worcester, MA, USA, 01605

28 [11] Lead contact

29 # denotes current affiliation

30 *Corresponding author: Amy H. Buck, a.buck@ed.ac.uk

31

32

Abstract

Argonautes are ancient proteins with well-characterised functions in cell-autonomous gene regulation and genome defense but less clear roles in non-cell-autonomous processes. Extracellular Argonautes have been reported across plants, animals and protozoa yet their biochemical and functional properties remain elusive. Here we demonstrate that an extracellular Argonaute (exWAGO) released by the rodent-infective parasitic nematode *Heligmosomoides bakeri* is detectable inside mouse cells during the natural infection. We further show that exWAGO is released from *H.bakeri* in both vesicular and non-vesicular forms that have different resistances to proteolysis, different accessibilities to antibodies and associate with different subsets of secondary siRNAs. Using recombinant exWAGO protein we demonstrate that non-vesicular exWAGO is directly internalised by mouse cells *in vitro* and that immunisation of mice with exWAGO confers partial protection against subsequent *H. bakeri* infection and generates antibodies that block exWAGO uptake into cells. Finally, we show that properties of exWAGO are conserved across Clade V nematodes that infect humans and livestock. Together this work expands the context in which Argonautes function and illuminates an RNA-binding protein as a vaccine target for parasitic nematodes.

Keywords: Argonaute, host-pathogen, extracellular RNA, RNA interference, nematode, parasite, RNA communication

Introduction

Argonautes are ancient proteins that work in partnership with small nucleic acid guides to regulate gene expression, control transposable elements and defend cells against viruses. In animals there are two highly conserved clades of Argonautes: the AGO family that acts with microRNAs (miRNAs) or short interfering RNAs (siRNAs), and the PIWI family that acts with PIWI RNAs (piRNAs) (Swarts *et al*, 2014). Nematodes have evolved an additional clade of Argonautes, the Worm-specific Argonautes (WAGOs), which bind secondary siRNAs that are generally 22 nucleotides in length, start with a Guanosine (G) nucleotide and commonly have a 5' triphosphate moiety due to their generation by RNA-dependent RNA polymerases (Gu *et al*, 2009; Seroussi *et al*, 2023; Yigit *et al*, 2006). Research in *Caenorhabditis elegans* suggests that WAGOs function to amplify or transmit

2

66 an RNA interference (RNAi) response, for example during environmental RNAi (amplifying

67 responses against foreign RNA) or soma-to-germline transmission of RNAi

68 (transgenerational inheritance) (Ketting & Cochella, 2020). However, many nematode

69 species are parasitic and how they might use Argonautes during infections inside diverse

70 hosts has not been well explored (Buck & Blaxter, 2013).

71 In order to survive in their hosts, parasitic nematodes release excretory-secretory (ES)

72 products that condition the host environment and immune response towards tolerance,

73 also promoting chronic infections (Maizels, 2020; Girgis *et al*, 2013; King & Li, 2018).

74 *Heligmosomoides bakeri* is a gastrointestinal nematode parasite of mice that serves as a

75 model for intestinal worm infections, which are estimated to affect a quarter of the world's

76 human population (WHO, 2023; Reynolds *et al*, 2012) and are highly prevalent in domestic

77 and wild animal species, causing substantial global health burdens and economic losses

78 (Charlier *et al*, 2020). We previously showed that extracellular vesicles (EVs) are a

79 component of *H. bakeri* ES (HES) and demonstrated that the parasite EVs have immune

80 suppressive properties in host cells (Buck *et al*, 2014; Coakley *et al*, 2017). We

81 subsequently discovered that a specific WAGO protein (Hb-exWAGO) is present in these

82 EVs in association with siRNAs (Chow *et al*, 2019). Yet whether EVs are the main carrier

83 of siRNAs and exWAGO is not clear, nor is it known whether Hb-exWAGO serves a

84 function during infection. Studies in plants have demonstrated that small RNA trafficking

85 from fungal or oomycete pathogens into plant cells is important for pathogen survival and

86 immune evasion (Qiao *et al*, 2023). Yet in these systems the pathogen small RNAs hijack

87 the Argonaute of the receiving host cell to function (Qiao *et al*, 2023). There is no example

88 to date of an Argonaute from one species operating in another, despite a mounting body

89 of literature across plants, protozoa and animals that Argonautes can get out of cells in

90 multiple forms (He *et al*, 2021; Geekiyanage *et al*, 2020; Arroyo *et al*, 2011; McKenzie *et*

91 *al*, 2016; Melo *et al*, 2014; Karimi *et al*, 2022; Si *et al*, 2023; Chow *et al*, 2019; Garcia-

92 Silva *et al*, 2013; Zhang *et al*, 2019, 2021; Jeppesen *et al*, 2019).

93 Here we take advantage of vaccination as a method to target the environment-exposed

94 form of Hb-exWAGO in *H. bakeri*. We show that vaccination with recombinant Hb-

95 exWAGO significantly reduces parasite burden and that antibodies raised during infection

96 block the uptake of non-vesicular Hb-exWAGO into cells *in vitro.* We also provide evidence

97 of transfer of the Hb-exWAGO from nematode to mouse cells during the natural infection

98   using immunohistochemistry. Finally, we show that the properties of exWAGO are

99   conserved in Clade V parasitic nematodes that infect humans and livestock, including high

100   expression in adult stages, presence in ES products and preference for binding secondary

101   siRNAs. This work illuminates the functional capacity of an extracellular Argonaute and

102   reveals a new vaccine candidate for an important and neglected class of pathogens where

103   there are no vaccines for humans (Perera & Ndao, 2021), limited (and no recombinant)

104   vaccine options in animals (Claerebout & Geldhof, 2020) and mounting resistance to

105   anthelminthic drugs (Orr *et al*, 2019; Wit *et al*, 2021).

106

Results

108

Non-vesicular and vesicular Hb-exWAGO both bind to secondary siRNAs but have

different accessibilities to proteases and antibodies

111   In order to isolate vesicular and non-vesicular forms of Hb-exWAGO we used sequential

112   centrifugation, filtration and ultracentrifugation of *H.bakeri* excretory-secretory products

113   (HES). Using western blot analysis, we found that Hb-exWAGO in EVs was largely

114   protected from proteolysis following proteinase K incubation in the absence of detergent

115   whereas Hb-exWAGO in EV-depleted HES was susceptible (Figure 1A). We then

116   developed an ELISA assay to test whether vesicular and non-vesicular Hb-exWAGO had

117   different accessibilities to antibody capture. Using equal total protein inputs from EVs and

118   EV-depleted HES, we detected an increase in the Hb-exWAGO signal when EVs were

119   treated with detergent, whereas the Hb-exWAGO signal in EV-depleted HES remained

120   unaffected (Figure 1B). These data collectively demonstrate that Hb-exWAGO is present

121   both inside and outside EVs with each form having different protease sensitivities and

122   antibody accessibilities. Using the ELISA assay in the presence of detergent with a

123   recombinant Hb-exWAGO standard we further quantified that approximately $8.2\pm1.0\mathrm{x}10^{6}$

124   (mean ± S.E.M) total copies of Hb-exWAGO are secreted per adult worm per day *ex vivo*

125   (Figure 1C). We note that EVs accounted for <5% of the total amount of protein found in

126   HES products when purified by ultracentrifugation (Figure S1A) and western blot analysis

127   confirmed that substantially more non-vesicular Hb-exWAGO is released by the parasites

128   compared to vesicular Hb-exWAGO (Figures 1D and S1B). We then carried out

129   immunoprecipitation of Hb-exWAGO to determine whether both the vesicular and non-

130   vesicular forms bind small RNAs. As shown in Figure 1E (upper panel), Hb-exWAGO

131   isolated from both EVs and EV-depleted HES binds to small RNAs that are largely 22-23

132   nucleotides (nt) in length and start with a Guanosine, features that are consistent with

133   secondary siRNAs (Chow *et al*, 2019). Consistent with our previous results using qRT-

134   PCR of small RNAs bound to Hb-exWAGO in EVs, the majority of Hb-exWAGO-bound

135   siRNAs in both EVs and EV-depleted HES derive from transposable elements (Chow *et*

136   *al*, 2019) (Figure 1E lower panel). Strikingly however, multidimensional scaling (MDS)

137   analysis shows that distinct siRNA populations are bound to Hb-exWAGO in EVs and EV-

138   depleted HES, and both of these are also distinct from the total population of siRNAs

139   bound to Hb-exWAGO within the adult worms (Figure 1F). Differential expression analysis

140   of the genomic regions producing the Hb-exWAGO-bound siRNAs indicates that 45,379

141   genomic regions produce more siRNAs in the EV-depleted HES, while 16,194 regions

142   produce more in EVs (Figure 1G). Collectively, these data demonstrate that Hb-exWAGO

143   exists in both vesicular and non-vesicular forms, that these are not contaminants of one

144   another, and that both forms are released in complex with distinct populations of siRNAs.

145

146   **Hb-exWAGO is detected inside host cells *in vivo* and internalised by live cells *in***

147   ***vitro***

148   The above data suggest the adult worms release large quantities of Hb-exWAGO *ex vivo*.

149   To test whether Hb-exWAGO is also released *in vivo* we used immunohistochemistry of

150   paraffin-embedded *H. bakeri*-infected mouse gut sections at 7 days post infection. As

151   shown in Figure 2A, Hb-exWAGO is detected inside the parasite, and also inside host

152   immune cells that surround the worm. These data show that substantial quantities of Hb-

153   exWAGO are detected *in vivo* and inside host cells, but do not distinguish which form of

154   Hb-exWAGO, vesicular and/or non-vesicular, is transmitted to host cells.

155   While we and others have shown uptake of parasite EVs by host cells, there is limited data

156   on the capacity of non-vesicular nematode parasite proteins to enter live host cells, and

157   no examples to date in this parasite model. We therefore first labelled EV-depleted HES

158   with Cy-5 NHS Ester dye and tested whether EV-depleted HES proteins are internalised

159   by mouse intestinal enterocyte epithelial MODE-K cells (Vidal *et al*, 1993). Signal was

160   detected by 4 hours post incubation and remained strong at 24 hours with accumulation

161   in the cytoplasm (Figure S2A). We then tested whether the recombinant Hb-exWAGO

162   itself could be internalised, using BSA as a control for non-specific uptake. We compared

163   uptake in the MODE-K cell line to a macrophage RAW 264.7 cell line expected to

164   phagocytose extracellular material. As shown in Figure 2B, we detect internalisation of

165   recombinant Hb-exWAGO by both MODE-K and RAW 264.7 cells, whereas BSA is only

166   internalised by the RAW 264.7 cell line. We further developed a Flow Cytometry assay

167   with MODE-K cells to measure recombinant Hb-exWAGO uptake down to picomolar

168   concentrations (Figure S2B). As shown in Figure 2C, there is a clear shift in the Median

169   Fluorescence Intensity in cells incubated with AF647-labelled Hb-exWAGO and near-

170   background signal from the AF647-labelled BSA and PBS controls (Figures 2C and S2C).

171   We note that cells were trypsinised to ensure any signal detected comes from internalised

172   labelled proteins and not those that could be associated to the surface. Taken together,

173   our results indicate that large quantities of Hb-exWAGO are released by adult parasites

174   and are detected inside host cells *in vivo*, and the non-vesicular form of Hb-exWAGO is

175   able to enter multiple cell types *in vitro* including epithelial cells.

176

Vaccination with recombinant Hb-exWAGO confers partial protection against

subsequent infection and generates antibodies that block Hb-exWAGO uptake into

cells

180   To understand whether the non-vesicular form of Hb-exWAGO might be important for

181   parasite survival in the host, we took advantage of the capacity to target this protein

182   through vaccination with recombinant Hb-exWAGO. We used, as a benchmark,

183   vaccination with total HES, which provides a cocktail of >360 proteins naturally released

184   by the parasite (Buck *et al*, 2014; Hewitson *et al*, 2015). HES vaccination in mice was

185   previously shown to result in sterile immunity with the observed effects attributed to both

186   IgG1 antibody-mediated and Type 2 cellular responses (Hewitson *et al*, 2015).

187   Mice were immunised with recombinant Hb-exWAGO, PBS (negative control) or HES

188   (positive control) in Imject Alum adjuvant followed by challenge with *H. bakeri* L3 stage

189   larvae (Figure 3A). As expected from previous studies (Hewitson *et al*, 2015; Coakley *et*

190   *al*, 2017), vaccination with HES confers sterile immunity as seen by a dramatic drop in the

191   number of eggs per gram of faeces at 14 days post-challenge and clearance of worms by

192   day 28 post-challenge compared to mice vaccinated with PBS (Figures 3B and C, and

193   S3A). Strikingly, vaccination with recombinant Hb-exWAGO resulted in an average

194   decrease of 67% in adult worm burdens compared to the PBS group at day 28 post-

195 challenge (Figures 3B and S3A). Consistent with the reduction in worm burden, there were

196 also decreased egg burdens, starting at day 14 post-challenge in the Hb-exWAGO-

197 vaccinated group (Figure 3C). Serum antibody responses show that vaccination with

198 recombinant Hb-exWAGO elicited IgG and, in particular, IgG1 antibodies specific to Hb-

199 exWAGO (Figures 3D and S3B), consistent with known effects of alum adjuvant (Boyaka,

200 2017). Immunisation with HES also induced generation of Hb-exWAGO-specific IgG1

201 antibodies, as expected since Hb-exWAGO is present in HES, but these are much lower

202 than in the Hb-exWAGO vaccine (Figure 3D). Interestingly, we detected Hb-exWAGO-

203 specific IgG1 antibodies post-challenge in mice immunised with PBS indicating that (at

204 least some of) the Hb-exWAGO protein becomes accessible to the immune system via

205 the natural secretion of Hb-exWAGO by the parasites and that lab mice naturally generate

206 a low level of Hb-exWAGO-specific antibodies during infection, but this is significantly

207 boosted by the vaccine (Figure 3D).

208 To test whether antibodies could inhibit Hb-exWAGO uptake by cells, we used the Flow

209 Cytometry assay with labelled recombinant Hb-exWAGO. As shown in Figure 3E,

210 treatment of MODE-K cells with sera from Hb-exWAGO vaccinated mice post-challenge

211 inhibited uptake of AF647-labelled Hb-exWAGO compared to sera from mice vaccinated

212 with HES and PBS. Reduction in the uptake of labelled Hb-exWAGO was also observed

213 by confocal microscopy following treatment of MODE-K cells with anti-Hb-exWAGO

214 antibodies compared to isotype controls (Figure S3C). These data suggest an antibody-

215 exposed form of Hb-exWAGO is important for parasite survival *in vivo* and demonstrate

216 that vaccination generates functional antibodies against Hb-exWAGO that block its uptake

217 into host cells.

218

ExWAGO is secreted across Clade V nematodes that infect livestock and humans
and shows conserved features in its association with 22G RNAs

221 A notable feature of Hb-exWAGO is its high conservation across Clade V gastrointestinal

222 nematodes that infect livestock and humans (spanning 65-81% amino acid identity,

223 Dataset S1). To examine whether these exWAGO orthologues have similar properties to

224 Hb-exWAGO, we first examined life stage expression of the exWAGO orthologues using

225 publicly available transcriptome data from *H. bakeri*, rodent-infective *Nippostrongylus*

226 *brasiliensis*, ruminant-infective *Teladorsagia circumcincta* and human-infective

7

227   *Ancylostoma ceylanicum* nematodes. As shown in Figure 4A and Dataset S2, exWAGO

228   expression is high in all the adult parasites, with lower levels in most larval stages across

229   the four species. Using the ELISA assay, we also found that *H. bakeri* adults (d14 p.c.)

230   release more Hb-exWAGO than larvae (d5 p.c.) and early adults (d7 p.c.) when using the

231   same volume of ES collected from equal numbers of larvae or adults, as shown in Figure

232   4B. Western blot analysis of ES from *T. circumcincta* also showed that more exWAGO is

233   found in ES from adults compared to larvae (Figure 4C). Furthermore, we detected

234   exWAGO in the ES of the ruminant- and human-infective worm *Trichostrongylus*

235   *colubriformis* and found it to be present in previously published proteomic analysis of the

236   ES of these parasites (Figure 4C and Table S1). Collectively our data suggest that

237   exWAGO is an abundant secreted protein expressed across the parasite developmental

238   stages and is most highly expressed in adults.

239   Given the high sequence conservation of exWAGO orthologues in these parasite species,

240   we tested whether antibodies generated against recombinant Hb-exWAGO could capture

241   exWAGO in the other parasites. Using western blot analysis, we show that exWAGO was

242   readily immunoprecipitated from *A. ceylanicum*, *N. brasiliensis* and *T. circumcincta*

243   (Figures 4D and E). We then compared the profile of small RNAs bound to exWAGO in

244   each species using small RNA sequencing and found that the small RNA profiles are

245   extremely similar, showing the expected Guanosine as the first nucleotide, a length of 22-

246   23 nucleotides and a propensity for mapping to transposable elements (Figure 4F).

247   Comparison between polyphosphatase-treated and untreated libraries also showed an

248   increase in the amount of small RNAs ligated to the adapters in response to 5' RNA

249   polyphosphatase treatment during the library preparation (Figure S4), consistent with the

250   presence of a 5' triphosphate. Taken together, these data strongly point towards functional

251   conservation of exWAGO orthologues in Clade V parasitic nematodes.

252

253   **Discussion**

254   This work provides the first evidence that an Argonaute protein (assumed mainly to

255   operate inside of cells) is a tractable vaccine candidate and suggests the non-vesicular

256   form of exWAGO is functionally relevant during nematode parasite infections. Vaccine

257   development remains challenging for parasitic nematodes, given the complex life cycles

258   of nematodes and the numerous mechanisms for immunomodulation that they have co-

8

259   evolved with their hosts over millions of years (Perera & Ndao, 2021). There are currently

260   only two licensed anti-nematode vaccines for animal use, both of which are limited in

261   scalability and rely on native antigens or irradiated larvae (Claerebout & Geldhof, 2020);

262   there are no licensed vaccines for humans despite growing resistance to anthelmintic

263   drugs (Perera & Ndao, 2021). Work by ourselves and others has demonstrated that

264   secreted RNAs are one type of immune evasion strategy used by nematodes (Buck *et al*,

265   2014; Liu *et al*, 2019; Tran *et al*, 2021; Ding *et al*, 2019) and we previously showed that

266   Hb-exWAGO is released in complex with secreted siRNAs in EVs (Chow *et al*, 2019). Here

267   we show a large proportion of Hb-exWAGO is released in a distinct non-vesicular form

268   and that vaccination against this protein reduces subsequent burdens of infection (67%

269   reduction in adult worm burdens) (Figure 3). As a single recombinant protein, this is

270   substantial compared to existing vaccines which often use a cocktail of antigens (Britton

271   *et al*, 2020), and its application could also be envisioned in multivalent strategies.

272   Our working hypothesis is that, by targeting Hb-exWAGO, we block a suite of small RNAs

273   from entering and acting within host cells and we show here that antibodies generated by

274   the vaccinations block recombinant Hb-exWAGO uptake by host cells *in vitro*. We cannot

275   rule out that antibodies could also target a form of Hb-exWAGO that is within the parasite

276   (for example if expressed and accessible to antibodies in the intestine) *in vivo*. However,

277   using a quantitative assay, we demonstrate that substantial (approx. 10^7) copies of Hb-

278   exWAGO are released by each parasite per day (Figure 1C) and show with

279   immunohistochemistry that Hb-exWAGO is clearly detected inside host cells during the

280   infection (Figure 2). We do not yet know the precise cells that internalise exWAGO or

281   whether Hb-exWAGO directly mediates gene silencing inside these cells. Hb-exWAGO

282   does not contain the catalytic DEDD/H tetrad involved in RNA slicing and still little is known

283   about the mechanism of gene silencing of the closest orthologs in *C. elegans*, SAGO-1,

284   SAGO-2 and PPW-1 that share approximately 30% amino acid identity with Hb-exWAGO

285   (Dataset S1). Based on its higher expression and release by adults, we speculate that Hb-

286   exWAGO plays an important role in the chronic infection stage, but it also could act earlier.

287   Our work interfaces with an increasing number of reports suggesting extracellular

288   Argonautes exist in multiple forms across plants and animals. In humans, these have been

289   reported within EVs (Bukong *et al*, 2014; Mantel *et al*, 2016; McKenzie *et al*, 2016) as well

290   as non-vesicular complexes including exomeres and supermeres (Jeppesen *et al*, 2019;

291 Zhang *et al*, 2019, 2021), and other non-vesicular forms (Arroyo *et al*, 2011; Geekiyanage

292 *et al*, 2020; Turchinovich *et al*, 2011). The dialogue around extracellular Argonautes has

293 primarily focused on whether Argonautes are genuinely packaged within EVs or represent

294 contaminants that co-purify (for example if associated with the surface of the EV) (Weaver

295 & Patton, 2020). We address this point specifically here with assays showing that

296 proteinase K sensitivity and antibody accessibility of the vesicular Hb-exWAGO occurs

297 only in the presence of detergent (in contrast to the non-vesicular form) (Figure 1). We

298 also show that the two forms of Hb-exWAGO bind to distinct subsets of secondary siRNAs.

299 A key message from this study is that non-vesicular extracellular Argonautes (in addition

300 to those within EVs) can also enter cells and this merits further understanding. The

301 mechanism(s) by which non-vesicular Hb-exWAGO could enter cells remains largely

302 unknown; there is only one study in this area that reports the human AGO2 can be

303 internalised into recipient cells via the receptor neuropilin-1 (Prud'homme *et al*, 2016).

304 Why the parasite releases two forms of Hb-exWAGO is not clear; we showed that Hb-

305 exWAGO from EVs versus EV-depleted HES bind secondary siRNAs derived from

306 different genomic locations. This suggests potentially different secretion origins within the

307 parasite and also possibly different gene targets in the host. It is also possible that having

308 two forms provides robustness to ensure some of the Hb-exWAGO will find its way into

309 the host cell. Given the ubiquity of extracellular Argonautes including in humans, our work

310 points to a need of better understanding the targeting properties and function of both

311 vesicular and non-vesicular forms of Argonautes across living systems.

312

313 **Materials and Methods**
314 **Ethics statement**

315 All the mice used in this project were bred by the inhouse facilities at The University of

316 Edinburgh. Experimental procedures were executed under a UK Home Office licence

317 P635073CF as approved by qualified veterinarians and were carried out by qualified

318 personnel in accordance with the UK Home Office guidelines.

319 **Recombinant exWAGO proteins**

320 The recombinant *H. bakeri* exWAGO and *T. circumcincta* exWAGO used in this

321 publication were produced by Sino Biological in insect cells and are 107.3 and 106.8 kDa

322 respectively. The recombinant proteins were designed to have 3x FLAG tags (underlined)

323 and a PreScission cleavage site (underlined and bold), followed by a 6x His tag

324 (underlined and italics) at the N-terminus as shown below.

325 The recombinant Hb-exWAGO protein sequence is as follows:
326 MDYKDDDDKDYKDDDDKDYKDDDDKAL**LEVLFQGP**ASG*HHHHHH*SGGGGSMDQLK
327 TGMGQLSVGAVALPEKRSPGGIGNKVDFVTNLTELSLKPNVPYYKYDIRMYIVYKGNDA
328 LEHLKELTKQTKDDFPEQERKSAAVAVYKHLCKTYKDVFLPDGALLYDRAAVLFSAQR
329 QLKLDGEEKQFMLPASVVSSAGPDATGIRVVIKKVKDQFQVTSNDLSKAVNVRDMERD
330 KGILEVLNLAVSQKGYMETSQFVTYGSGVHYLFDHRALGFRDNELPELMDGKYMGIGL
331 TKSVKVLEGDSGKGNSAFVVTDVTKGAFHVDEQNLMEKISQMSIFFDQRTGQSSFNAK
332 NAMQPFNQKAILQQIKGLYVRTTYGKKKTFPIGNLAAAANALKFQTADGAQCTVEQYFK
333 KHYNIQLKYPGMFTVSERHNPHTYYPVELLTVAPSQRVTLQQQTPDQVASMIKASATLP
334 QTRLHQTKIMKDALDITPRNHNLATAGISVANGFTAVSGRVLPSPRIAYGGNQILRPVDN
335 CKWNGDRSVFLEPAKLTNWAVCVTLTQQDARRLQIKEYISRVEMRCRNRGMQVDPVA
336 EVFTLKHQTFDGLKEWYASQKQKNRRYLMFITSDGIKQHDSIKLLEVEYQIVSQEIKGSK
337 VDAVVTKNQNQTLDNVVAKINMKLGGVNYNVMLGVKNDDKAFSWLNDKDRMFVGFEI
338 SNPPALSKVEIERGASYKMPSVLGWGANCAGNHQQYIGDYVYIQPRQSDMMGAKLSE
339 LIVDILKRFRAATTIAPRHIVLYFSGISEGQFSLVTDTYMRAVNTGIASLSPNYKPSVTAVA
340 VSKDHNERIYKTNISGNRATEQNIPPGTVIDTKIVSPVINEFYLNSHSAFQGTAKTPKYSL
341 LADNSKIPLDVIEGMTHGLCYLHEIVTSTVSVPVPLIVADRCAKRGHNVYIANSNQGEHS
342 VNTIDEANAKLVNDGDLKKVRYNA.

343 The recombinant *T. circumcincta* exWAGO protein sequence is as follows:
344 MDYKDDDDKDYKDDDDKDYKDDDDKAL**LEVLFQGP**ASG*HHHHHH*SGGGGSMADQL
345 SGGMGKLSVAAVALPEKRAPGSLGTKLDFVTNLTGIKLKPNVPYYKYDVRMYIVYKGND
346 GREVLKELTKQTKDDFPEQERKMAAVAIYKHLVKSYKDIFPQDGQFFYDRAAVLFSAQR
347 EMKLGGPEKVITLPASLSPTAGSDAAGIRVVIKKVTDGYQVTSNDLMKAVNVRDCERDK
348 GILEVLNLAVSQKGYMETSQFVTYGTGVHYLYDHRALGFRDNELPDLMDGKYMGIGLT
349 KAVKVLEGDQGKSASAFVVTDVTKGAFHIDEQNLLEKISQMSIFFDPRTGQSTFSVKAA
350 MQPHNMKSILQLIKGLYVRTTYGRKRTFPIGNLAAAPNALKLQTSDGVQCTIEQYFKKQ
351 YNVQLKYPGLFTVSERHNPHNYYPVELLTVAPSQRVTLQQQTPDQVASMIKASATLPS
352 NRLHQTKVMKEALDITPRNAKLASAGINVEDGFTTVPGRVLPTPTILYGGSQTLKPVDN
353 CKWNGDRSRFLEPAQLTNWAVCATLTQNDARRLQIKDYVARVESRCRAKGMQVEAAA
354 EIFTLTKQNFDGLREFYAAQKKKNRKYLLFITSDGIKQHDLIKLLEVEYQIVSQEVKGSKV
355 DSVMFKNQNQTLDNVIAKINMKLGGVNYNVVLGSKPNDPASKWLNDKDRLFVGFEISN
356 PPALSKMEIERGATYKMPSVLGWGANCAANPQHYIGDYVYIKPRQSDMMGAKLSELIV
357 EILKKFRGATSLAPRHIVLYFSGISEGQFSLVTDTYMKAINTGITSLSANYRPSVTALAVS
358 KDHNERLYKSNISGSRANEQNIPPGSVVDTKIVSPVINEFYLNSHSAFQGTAKTPKYSLL
359 ADDSKIPLDVIEGMTHGLCYLHEIVTSTVSVPVPLIVADRCAKRGHNIFIANSNLGSAAVS
360 SIEEANEKLVNHGELEKVRYNA.

361 **Parasite life cycle and collection of excretory/secretory products *H. bakeri***

362 For maintaining the life cycle of *H. bakeri*, CBA × C57BL/6 F1 male mice were infected

363 with 400 *H. bakeri* L3 stage larvae by oral gavage and adult worms were harvested from

364 the small intestine 14 days post-challenge. Adult worms were extensively washed and

365 cultivated in serum-free media (RPMI 1640 supplemented with 1.2% glucose, 5 U/ml

366   penicillin, 5 μg/ml streptomycin, 2mM L-glutamine and 1% gentamycin) as described in

367   Johnston et al, (2015). For collection of the excretory/secretory products from *H. bakeri*

368   (HES), the conditioned medium was collected on day 4 and 8 post-culture, however, the

369   first 24 hours of culture medium was first removed to reduce any potential host

370   contamination. The HES collected was spun (300 rcf, 5 min, room temperature) to remove

371   eggs, filtered (0.22 μm Millex-GP filter), and stored at -20°C until required. HES (~50-60

372   ml per batch of HES; batch is defined as the parasites collected and pooled from one

373   group of infected mice) was concentrated to <12.5 ml using a 5 kDa Vivaspin (3,000 rcf,

374   4°C) (GE Healthcare). Concentrated HES was then subjected to ultracentrifugation

375   (100,000 rcf, 70 min, 4°C) in polyallomer centrifuge tubes (Beckman Coulter) in a SW40

376   Ti swinging-bucket rotor (Beckman Coulter). The supernatant (SUP, also known as "EV-

377   depleted HES") was collected and concentrated to a final volume of 0.4-1.0 ml after buffer

378   exchange in > 40 ml of PBS using a 5 kDa Vivaspin (3,000 rpm, 4°C) (GE Healthcare).

379   The EV pellet was washed twice with 12.5 ml of cold PBS and spun as before. PBS

380   washes were discarded, and the EV pellet was resuspended in 120-150 μl PBS. The

381   protein concentration of EVs and EV-depleted HES was measured using the Qubit Protein

382   Assay kit (Thermo Fisher Scientific) and the material was stored at -80°C until required.

383   The number of particles in the purified EVs was measured using the ZetaView

384   Nanoparticle Tracking Analysis (Particle Metrix) as per manufacturer's instructions.

385   ***N. brasiliensis***

386   The *N. brasiliensis* life cycle was maintained by infection of Sprague-Dawley male rats

387   with 3,000 infective L3 larvae. Adult worms were obtained 8 days later from small intestinal

388   tissues in a Baermann apparatus as described in Lawrence et al, (1996). Worms were

389   washed extensively in PBS, and stored at -80°C until required.

390   ***A. ceylanicum***

391   *A. ceylanicum* hookworm life cycle was maintained in hamsters (Hu *et al*, 2012, 2018). All

392   housing and care of laboratory animals used in the hookworm study conform to the

393   National Institutes of Health (N.I.H., U.S.A.) Guide for the Care and Use of Laboratory

394   Animals in Research (see 18-F22) and all requirements and all regulations issued by the

395   United States Department of Agriculture (U.S.D.A.), including regulations implementing

396   the Animal Welfare Act (P.L. 89–544) as amended (see 18-F23). Adult worms were

397   collected from the gut of hamsters at day 20 post-infection. Following extensive washes

398   with Hanks' Balanced Salt Solution, worms were frozen at -80°C until used.

399   ***T. circumcincta* and *T. colubriformis***

400   For maintaining the life cycle of *T. circumcincta and T. colubriformis,* helminth-free lambs

401   (<6 months old) were orally infected with L3 stage parasites. For generation of L4 and

402   adult parasites animals were orally challenged with 150,000 or 20,000 L3 stage larvae,

403   respectively. Parasites at L4 stage (7 days post-infection) and adult stage (28 days post-

404   infection) were harvested from either the sheep gastric stomach (for *T. circumcincta*) or

405   the first 3 meters of the small intestine (for *T. colubriformis*). Worms were washed three

406   times in PBS and then cultured in RPMI 1640 medium (Thermo Fisher Scientific)

407   containing 20 mM HEPES pH 7.5, 1% (*w/v*) d-glucose, 2 mM L-glutamine, 1000 U/ml

408   penicillin, 1000 µg/ml streptomycin, 200 µg/ml gentamycin and 25 µg/ml amphotericin B,

409   at 37°C in 5% CO_2. Culture conditioned media were harvested every 24 hours and

410   replaced with fresh media, with worms maintained in culture for 120 hours post collection.

411   At each supernatant collection, parasite viability was confirmed on the basis of structural

412   integrity and motility.

413   Following collection, the culture supernatants were clarified by centrifugation at 300 rcf for

414   10 min at 4°C, filtered through a 0.2-µm Minisart syringe filter (Sartorius) and stored at -

415   70°C. For processing of excretory-secretory (ES) products, culture supernatants from all

416   collections were pooled then concentrated and buffer exchanged into PBS using 10-kDa

417   MWCO Amicon Ultra-15 Centrifugal Filter Units (Millipore Sigma), following the

418   manufacturer's guidelines. Protein concentration was determined using the Pierce™ BCA

419   protein assay (Thermo Fisher Scientific) with bovine serum albumin standards, and

420   aliquots of ES products were stored at -70°C prior to use.

421   **Cell culture**

422   The immortalised intestinal epithelial MODE-K cell line (derived from the small intestine of

423   C3H/He female mice) was kindly provided by Dominique Kaiserlian (French Institute of

424   Health and Medical Research) and were cultured at 37°C with 5% CO_2 in DMEM medium

425   supplemented with fetal bovine serum (10%), L-glutamine (1%), penicillin/streptomycin

426   (1%), sodium pyruvate (1%) and non-essential amino acids (1%) (Vidal *et al*, 1993). The

427   murine macrophage RAW 264.7 cell line (ATCC) was cultured at 37°C with 5% CO_2 in

428 DMEM medium supplemented with fetal bovine serum (10%), L-glutamine (1%), and
429 penicillin/streptomycin (1%).

Proteinase K treatment

431 *H. bakeri* EVs and EV-depleted HES (2.0 µg of protein) were treated with or without Triton
432 X-100 treatment (0.05%, 30 min, on ice), followed by Proteinase K digestion (5 µg/ml, 30
433 min, 37°C) (Epicentre) as appropriate. The reaction was quenched by addition of
434 phenylmethanesulfonyl fluoride (5 mM, 1h, on ice) (Sigma). Samples were then prepared
435 for western blot analysis.

Western Blot analysis

437 Protein samples were reduced and separated on 4-12% Bis-Tris NuPAGE SDS gels
438 (Thermo Fisher Scientific). The separated proteins were transferred on an Immobilon-FL
439 PVDF membrane (Millipore) by wet transfer (100V, 105 min). The membrane was blocked
440 and then incubated with the primary antibody (4°C, overnight, on roller). For detection of
441 Hb-exWAGO protein a polyclonal rabbit antibody generated and purified against the
442 peptide TKQTKDDFPEQERK (Eurogentec) was used at 1:4,000 in 5% BSA/0.1% TBST
443 (Chow *et al*, 2019), unless otherwise specified. For detection of exWAGO orthologues in
444 ES from *T. circumcincta* and *T. colubriformis,* a mouse monoclonal antibody (clone C5F7)
445 generated in house as described in Hewitson et al, (2011) against recombinant Hb-
446 exWAGO was used at 1:2,000 in 3% milk/0.1% TBST. Following incubation with primary
447 antibodies, the membrane was incubated (1h, room temperature) with goat anti-rabbit IgG
448 DyLight 800 (Thermo Fisher Scientific, SA5-35571) or goat anti-mouse IgG AF680
449 secondary antibodies (Thermo Fisher Scientific, A21058). The signal was visualised using
450 the Odyssey CLx imaging system (LICOR) and band intensities were quantified using
451 ImageJ (Fiji) as described in Stael et al, (2022).

ELISA for detection and quantification of native Hb-exWAGO protein

453 Secreted Hb-exWAGO from EVs, EV-depleted HES and total HES was measured using
454 ELISA. Immuno plates (Thermo Fisher Scientific) were coated with polyclonal rat anti-Hb-
455 exWAGO antiserum capture antibody (raised against recombinant Hb-exWAGO in-house)
456 in 0.06 M carbonate buffer (4°C, overnight) and blocked (4% BSA/TBS, 37°C, 2h).
457 Samples were lysed as required with 0.05% Triton X-100 (30 min, on ice), and plated (4°C,

14

overnight) in dilution buffer (1% BSA/TBST). For detection, the polyclonal rabbit UE3R2 anti-exWAGO primary antibody (produced by Sino Biological against recombinant Hb-exWAGO) was used (5 µg/ml in dilution buffer, 2h, room temperature) followed by incubation with goat anti-rabbit IgG-HRP (Cell Signalling, 7024S) secondary antibody (1:2,000 dilution, 37°C, 1h, in the dark). The reaction was developed using TMB substrate buffer (SeraCare), stopped (10% phosphoric acid), and the optical density was read at 450 nm on the Varioskan Flash (Thermo Fisher Scientific). Samples were analysed in technical duplicates and wells with buffer only (no sample) were used to determine the background signal.

For quantification of Hb-exWAGO, a standard curve with recombinant Hb-exWAGO with 0.05% Triton X-100 in dilution buffer was prepared in a four-fold serial dilution (from 0.01907 pg to 20 ng), and analysed using a 4PL regression (GraphPad Prism). The amount of Hb-exWAGO was interpolated using the optical density values obtained in the ELISA assay. The limit of detection was calculated from 5 independent experiments as the mean of blanks + (standard deviation of blanks * 3.3) and the limit of quantification was calculated as the mean of blanks + (standard deviation of blanks * 10).

For detection of Hb-exWAGO secreted at different *H. bakeri* life stages, female C57BL/6 mice were infected with 200 L3 stage larvae by oral gavage. At day 5, 7 and 14 post-challenge mice were culled and larvae or adult worms were collected from the gut wall or lumen of the small intestine respectively. Larvae were washed 5x with Hanks' Balanced Salt Solution supplemented with penicillin-streptomycin (1%). Adult worms were treated with gentamycin (1 mg/ml) in Hanks' Balanced Salt Solution supplemented with penicillin streptomycin (1%). Worms were then visually inspected for motility and any obvious injuries and were cultivated in groups of 20 in a 48-well plate with 500 µl serum-free culture media. The first 24 hours of culture medium was removed and replenished. HES was collected and replenished 2 and 4 days after culture. For the ELISA assay, day 2 and 4 HES were pooled by equal volume and tested directly (i.e., no PBS exchange), while culture medium only samples were used as a negative control.

For quantification of Hb-exWAGO secreted by adult worms harvested at day 14 post infection: Worms were cultivated in groups of 30 (15 male and 15 female as determined by visual inspection) in a 24-well plate with 400 µl serum-free culture media. The first 24 hours of culture medium was removed, replenished, and HES was collected 4 days post

15

490   culture. The HES collected was tested directly (i.e., no PBS exchange) by ELISA, and

491   culture medium only samples were used as negative control.

Uptake of non-vesicular proteins

493   To examine if non-vesicular proteins are internalised by epithelial cells *in vitro*, proteins in

494   EV-depleted HES or PBS were labelled using a Cy5 NHS Ester dye (AAT Bioquest, 151)

495   according to the manufacturer's instructions at a 15:1 (dye to protein) molar ratio.

496   Unconjugated dye was removed using the Zeba 7K MWCO spin columns (Thermo Fisher

497   Scientific, 89882) as per manufacturer's instructions. The labelled EV-depleted HES and

498   PBS were stored (-80°C, dark) until required. MODE-K cells (1.5×10^5) were seeded in a

499   24-well plate with 400 µl MODE-K media overnight. The cells were treated with Cy5-

500   labelled EV-depleted HES at a final concentration of 10 µg/ml or 50 µg/ml or with an

501   equivalent volume of Cy5-labelled PBS as a negative control for 4 or 24 hours. The cells

502   were washed twice with PBS, supplemented with fresh media, and imaged on the EVOS

503   M7000 Imaging system (Invitrogen) with the EVOS LED Light Cube Cy5 2.0 using the

504   EVOS 60x objective, fluorite, LWD. Data were analysed on the EVOS Analysis software

505   v1.5.1479.304.

Immunohistochemistry

507   To detect Hb-exWAGO *in vivo*, C57BL/6 female mice were infected with 200 L3 stage

508   larvae by oral gavage. At day 7 of infection, mice were culled and the upper half of the

509   small intestine was removed for preparation into a gut roll. Fat was trimmed away from the

510   gut wall and the intestines were rolled inside-out onto wooden skewers. The intestines

511   were fixed for 30 minutes in 4% PFA (diluted from 16% methanol-free PFA, VWR). The

512   intestines were cut lengthwise and rolled onto a new skewer as 'gut rolls', then incubated

513   for a further 5 hours in fresh 4% PFA. The gut rolls were washed twice in PBS and then

514   stored overnight in 70% ethanol before processing sequentially in 80% ethanol (30 min),

515   95% ethanol (30 min, twice), 100% ethanol (30 min, twice), xylene (30 min, twice), and

516   paraffin wax (40 minutes at 60°C), before embedding in paraffin wax. 10 µm sections were

517   cut from the resulting blocks, which were mounted on Superfrost Plus slides (VWR), dried

518   overnight, baked for one hour at 60°C and stored at 4°C. Wax was removed for staining

519   by washing sequentially in xylene (3 min, twice), xylene/ethanol mixed 1:1 (3 min), 100%

520   ethanol (3 min, twice), 95% ethanol (3 min), 70% ethanol (3 min), 50% ethanol (3 min),

521 before a final rinse with water. Antigen retrieval involved a 30-minute treatment in citrate

522 buffer (Abcam) in a 98°C water bath, before a further 20-minute cool-down outside the

523 water bath. Slides were washed in TBS and then blocked using TBS buffer with 1% BSA

524 and 0.1% Tween-20. For Hb-exWAGO detection, 2.5 µg/mL of rabbit anti-Hb-exWAGO

525 antibody UE3R2 or the polyclonal rabbit IgG isotype-matched control antibody (Thermo

526 Fisher Scientific, 02-6102) were incubated on the slides overnight in TBS buffer with 0.1%

527 Tween-20 at 4°C. After washing three times in TBS buffer with 0.1% Tween-20, Alexa

528 Fluor 647 anti-rabbit secondary antibody (diluted 1:2,000 in TBS with 0.1% Tween-20)

529 (Thermo Fisher Scientific, A21245) was incubated on the slides for two hours at room

530 temperature. DAPI diluted 1:1,000 was added to the slides and washed off twice in TBS

531 before mounting in ProLong Gold (Thermo Fisher Scientific). The slides were imaged on

532 a Zeiss LSM 980 microscope with Airyscan 2 detector, using the Zeiss 20x 0.8 NA Air

533 objective, with 405 and 639 nm lasers. Data were acquired using the Zen Blue 3.5 (Zeiss)

534 and processed using Zen Blue 3.3 software (Zeiss).

535 **Uptake and blockade of recombinant Hb-exWAGO**

536 To test whether non-vesicular Hb-exWAGO is internalised by epithelial and macrophage

537 cells *in vitro*, equimolar amounts of recombinant Hb-exWAGO, BSA and PBS were

538 labelled with AF647 NHS Ester dye (Thermo Fisher Scientific, A37573) according to the

539 manufacturer's instructions at a 15:1 (dye to protein) molar ratio. Unconjugated dye was

540 removed using the Zeba 7K MWCO spin columns (Thermo Fisher Scientific, 89882) as

541 per manufacturer's instructions. The labelled proteins and PBS were stored (-80°C, dark)

542 until required.

543 To assess the uptake of AF647-labelled Hb-exWAGO by mouse cells using confocal

544 microscopy, 1.0×10^4 MODE-K or RAW 264.7 cells were seeded in an 18-well ibidi-treat µ-

545 slide (Ibidi, 81816) in 100 µl culture medium overnight. The cells were incubated (37°C

546 with 5% CO_2) with 0.1 µM Hb-exWAGO, BSA, or PBS labelled with AF647 NHS Ester for

547 4 hours. For blocking the uptake of Hb-exWAGO in MODE-K cells, anti-Hb-exWAGO rat

548 serum (produced in-house against recombinant Hb-exWAGO as described in Chow et al.

549 (Chow *et al*, 2019)) or naïve rat serum were added at a 1:167 final dilution mixed with the

550 labelled protein. Following incubation, the cells were washed twice with PBS, fixed with

551 4% PFA (10 min), washed again, stained with DAPI, washed again, and mounted using

552 the ibidi mount medium (Ibidi, 50001). Slides were stored (4°C, dark) and imaged within

17

553 three days of preparation. The samples were illuminated with 405 and 639 nm lasers and

554 imaged on the Zeiss laser scanning confocal microscope LSM 980 with Airyscan 2

555 detector using the Zeiss 63x 1.4 NA Oil objective. Data were acquired using the Zen Blue

556 3.5 (Zeiss) and processed using the Zen Blue 3.3 software (Zeiss).

557 To assess the uptake and blocking of AF647-labelled recombinant Hb-exWAGO by mouse

558 cells using flow cytometry, 0.8×10^5 MODE-K cells were seeded in a 24-well plate in 500

559 μl culture medium overnight. The cells were incubated (37°C with 5% CO_2) with 10 nM of

560 AF674-labelled Hb-exWAGO, BSA, or PBS for 4 hours. For blocking the uptake of

561 recombinant Hb-exWAGO in MODE-K cells, sera obtained from Hb-exWAGO-, HES-, or

562 PBS-vaccinated mice were added to the cells at a 1:250 final dilution directly prior to

563 addition of AF647-Hb-exWAGO. Following incubation, the cells were washed twice with

564 PBS, trypsinised (5 min, at 37°C with 5% CO_2), resuspended in 5% FBS/PBS and

565 centrifuged (400 rcf, 5 min, room temperature). The cells were resuspended in 0.5%

566 FBS/PBS and analysed on the MACSQuant Analyser 10 (Miltenyi Biotec) using the R1

567 channel. Data were analysed using FlowJo software v10.

568 **Immunisation of mice**

569 For vaccine experiments, female C57BL/6 mice between 7-12 weeks old were immunised

570 intraperitoneally with recombinant Hb-exWAGO or PBS or HES in Imject alum adjuvant

571 (Thermo Fisher Scientific) at 1:1 volume ratio (total intraperitoneal injection volume was

572 200 μl). Mice were primed (10 μg) and boosted (2 μg) twice at 28 and 35 days post priming

573 as described in Hewitson et al, (2015). 7 days following the second boost, the mice were

574 challenged with 200 *H. bakeri* L3 stage larvae by oral gavage. Mice were culled 14 and

575 28 days post-challenge by CO_2 overdose or by intraperitoneal administration with Dolethal

576 (30 mg, Vetoquinol). We note that a prolonged period of 3 months between priming and

577 the first boost occurred for one of the three independent experiments due to COVID-19

578 interruptions.

579 The small and large intestine were carefully removed, stretched and the number of adult

580 worms counted. The number of eggs was measured using the McMaster Egg Counting

581 Chamber (CellPath) following floatation with saturated sodium chloride solution as

582 described in Camberis et al, (2003). The blood serum was acquired via tail bleed or for

583 euthanised mice it was collected using cardiac puncture. The blood was incubated (1-2

18

584   hours, room temperature) and centrifuged (5,000 rcf, 5 min, room temperature). The

585   supernatant containing the serum was centrifuged again as before and stored at -80°C

586   until required.

ELISA for measuring Hb-exWAGO-specific antibody responses

588   Hb-exWAGO-specific serum antibody responses were measured using an Enzyme-

589   Linked Immunosorbent Assay (ELISA). Plates were coated with 0.05 µg of recombinant

590   Hb-exWAGO (Sino Biological) in 0.06 M carbonate buffer (4°C, overnight), blocked (4%

591   BSA/TBS, 37°C, 2h), and blood serum was plated in a two-fold serial dilution (4°C,

592   overnight) in dilution buffer (1% BSA/TBST). The secondary antibodies goat anti-mouse

593   IgG1-HRP (SouthernBiotech, 1070-05) or goat anti-mouse IgA-HRP (SouthernBiotech,

594   1040-05) were used (1:2,000 dilution, 37°C, 1h, in the dark). The reaction was developed

595   using TMB substrate buffer (SeraCare), stopped (10% phosphoric acid), and the optical

596   density was read at 450 nm on the Varioskan Flash (Thermo Fisher Scientific). Samples

597   were analysed in technical duplicates and wells without sample were used to determine

598   the background signal.

exWAGO immunoprecipitation

600   exWAGO was immunopurified using polyclonal rat anti-exWAGO serum (generated in-

601   house against the *H. bakeri* or *T. circumcincta* recombinant exWAGO protein) or naive rat

602   serum antibodies conjugated to Protein G magnetic beads (Thermo Fisher Scientific,

603   10003D). In all immunoprecipitations, *H. bakeri* anti-exWAGO rat serum was used except

604   for pull-downs from *T. circumcincta* worms where *T. circumcincta* anti-exWAGO rat serum

605   was used as this was available. Beads were washed five times in cold Binding Wash Buffer

606   (PBS, 0.02% Tween-20) and the antibodies were then conjugated on the washed beads

607   by incubation (2h, 4°C, rotating wheel). Unconjugated antibody was then removed, and

608   the beads were equilibrated with the appropriate lysis buffer three times.

609   To immunoprecipitate exWAGO and its orthologues from adult worms, nematodes were

610   lysed by bead beating (5 mm steel bead, Qiagen) using the Tissue Lyser II (Qiagen) in

611   pre-cooled cartridges for 2 min at 30 Hz twice in worm lysis buffer (150 mM NaCl, 10 mM

612   Tris.HCl, 0.5 mM EDTA, 0.5% NP40) containing protease and phosphatase inhibitors (1

613   tablet per 5 ml, Roche), and 200 U/ml RNase inhibitors (Promega). Unlysed material was

614   removed by centrifugation (16,100 rcf, 10 min, 4°C). The supernatant containing lysed

615   worms was quantified using the Qubit Protein Assay kit (Thermo Fisher Scientific). Per

616   immunoprecipitation, 150 µg of adult worm lysate protein was used.

617   To identify the small RNAs associated with the vesicular and non-vesicular Hb-exWAGO,

618   we immunoprecipitated Hb-exWAGO from EV and EV-depleted HES derived from

619   corresponding batches, using 10X more EVs by protein weight to account for lower

620   amounts of exWAGO in EVs compared to EV-depleted HES: EVs (17 µg of protein) or

621   EV-depleted HES (170 µg of protein) were lysed (20 min, on ice) in TBS/0.05% Triton X-

622   100 with protease inhibitors (1 tablet per 10 ml, Roche) and 200 U/ml RNase inhibitors

623   (Promega).

624   The lysate was incubated with the antibody-conjugated beads (45 min, 4°C, rotating

625   wheel). The beads were washed with cold Low Salt buffer (50 mM Tris.HCl pH 7.5, 300

626   mM NaCl, 5 mM MgCl$_2$, 0.5% Triton X-100 and 2.5% glycerol), followed by two washes

627   with cold High Salt buffer (50 mM Tris.HCl pH 7.5, 800 mM NaCl, 10 mM MgCl$_2$, 0.5%

628   Triton X-100 and 2.5% glycerol) for 5 min at 4°C, using a rotating wheel. The beads were

629   washed once more with Low Salt buffer, followed by a cold PNK buffer wash (50 mM

630   Tris.HCl pH 7.5, 50 mM NaCl, 10 mM MgCl$_2$, 0.5% Triton X-100). For western blot analysis

631   proteins were eluted in denaturing buffer whereas for small RNA sequencing analysis the

632   RNA was eluted directly in Qiazol (700 µl, 5 min, room temperature) (Qiagen).

Small RNA libraries

634   RNA in Qiazol (Qiagen) was spiked with 7 µl of 10 pM RT4 synthetic spike

635   (CTTGCGCAGATAGTCGACACGA) and extracted using the miRNA Serum/Plasma kit

636   (Qiagen) according to the manufacturer's instructions. The purified RNA was treated with

637   RNA 5' Polyphosphatase (Lucigen) according to the manufacturer's instructions. The

638   reaction was terminated by ethanol precipitation (-70°C, overnight) and the precipitated

639   RNA was resuspended in 2.5 µl of nuclease-free water and 2.5 µl of Buffer 1 (TriLink, L-

640   3206). The small RNA libraries were prepared using the CleanTag Small RNA Library

641   Preparation Kit (TriLink, L-3206) according to the manufacturer's instructions using half

642   reaction volumes. All libraries were generated using 1:12 dilution of 5' and 3' adapters with

643   20 amplification cycles. The profile of each small RNA library prior to sequencing was

644   assessed using either Novex 6% TBE acrylamide gels (Thermo Fisher Scientific) or the

645   High Sensitivity DNA Bioanalyser chip (Agilent). Pooled libraries were size selected (140-

646   220 bp for libraries made from adult worms or 140-180 bp for EV and EV-depleted HES

647   libraries) using gel purification to remove adapter dimers. The libraries were sequenced

648   on the Illumina NextSeq 2000 platform by the Edinburgh Clinical Research Facility or on

649   the Illumina NovaSeq 6000 by Edinburgh Genomics using single-end 100 base pair reads.

650   **Small RNA bioinformatic analysis**

651   The raw sequencing data were checked using FastQC v.0.12.1 and MultiQC v.1.14

652   (Andrews, 2010; Ewels *et al*, 2016) with no issues identified. The 3' adapter sequence

653   (TGGAATTCTCGGGTGCCAAGG) was removed using the Reaper tool from the Kraken

654   package (Davis *et al*, 2013), and 18-27 nt reads were retrieved using Pullseq (available

655   at: https://github.com/bcthomas/pullseq). ShortStack v.3.8 (Johnson *et al*, 2016) was then

656   used to align reads to their respective genome, allowing up to one mismatch and weighted

657   assignment of multi mapping reads (--nohp --mincov 5 --pad 1 --mismatches 1 --mmap u

658   --bowtie_m all --ranmax 'none'). Count matrices were prepared across all samples, as well

659   as plots showing the length distribution and first nucleotide preference, using the

660   01.featureCounts.R, 02.get_fn_mtx.R and 03.fn_long_cpm.R R scripts (available at:

661   https://github.com/imu93/exwago_vaccine). Count values were transformed to counts per

662   million (CPM) using the cpm function from the edgeR R package (Robinson *et al*, 2010).

663   The data are deposited to the NCBI Sequence Read Archive (SRA) under the BioProject

664   ID PRJNA1200757.

665   **Differential expression analysis of Hb-exWAGO immunoprecipitation from EVs and**

666   **EV-depleted HES**

667   Count matrices were first filtered to remove regions with less than five CPMs using the

668   filterByExpr function from the edgeR (Robinson *et al*, 2010). The Trimmed Mean of M-

669   values (TMM) normalisation and glmFit test were then used to estimate normalisation

670   factors and fit negative binomial generalised log-linear models, respectively. The glmTreat

671   test was used to identify regions significantly enriched in each secreted Hb-exWAGO form

672   (Fold-change threshold = 2).

673   **Identification of exWAGO orthologues and Protein sequence alignment**

674   Given the release of new genome assemblies for Strongylida parasites since the curation

675   of exWAGO annotations (Chow *et al*, 2019), gene and protein exWAGO annotations of

676 each genome were updated using miniprot (Li, 2023). Where available, the curated

677 exWAGO protein was used. In cases where no curated exWAGO for that species was

678 available, the sequence of the most closely related species was used for gene and protein

679 prediction (e.g. *T. colubriformis* and *T. circumcincta*). Amino acid identity was further

680 calculated using BLASTp against Hb-exWAGO annotated in the nHp.2.0 assembly (Chow

681 *et al*, 2019).

RNA sequencing data analysis

683 RNA-seq data was downloaded from NCBI SRA for the following species: *H. bakeri*

684 (PRJNA750155), *N. brasiliensis* (PRJNA994163 and PRJEB20824), *T. circumcincta*

685 (PRJEB7677) and *A. ceylanicum* (PRJNA231490). FastQC v.0.12.1 and MultiQC v.1.14

686 were used for quality control (Ewels *et al*, 2016; Andrews, 2010). Although almost all

687 libraries showed no quality issues, those corresponding to the PRJNA994163 *N.*

688 *brasiliensis* showed high proportions (~15%) of Clontech SMART Primer II sequence and

689 Illumina universal adapter. Thus, for these libraries an extra trimming step was

690 implemented with cutadapt v.4.9 and parameters -g ^AAGCAGTGGTATCAAC -G

691 ^AAGCAGTGGTATCAAC -m.

692 The selected RNA-seq reads were aligned to their respective genome using STAR

693 v.2.7.10b with the gtf gene annotation files to define junctions (--sjdbGTFfile

694 gtf_annotation_file   --clip3pAdapterSeq   AGATCGGAAGAGCACACGT

695 AGATCGGAAGAGCGTCGTG --outFilterMismatchNmax 3 --outFilterScoreMinOverLread

696 0.3) (Dobin *et al*, 2013). After alignment, gene expression was quantified using the

697 featureCounts function from the Rsubread R package (Liao *et al*, 2019)

698 (allowMultiOverlap= TRUE, requireBothEndsMapped = TRUE, countChimericFragments

699 = FALSE, useMetaFeatures=TRUE, fraction = TRUE). The resulting raw counts were

700 normalized into Transcripts Per Million (TPM) using the convertCounts function from the

701 DGEobj.utils R package (Thompson *et al*, 2022). Each biological replicate was treated

702 individually. If more than one orthologue was identified, the gene locus with the highest

703 mapped reads and highest percentage amino acid identity was used (Dataset S1 &

704 Dataset S2).

Statistical analysis

Data were checked for normality using the Shapiro-Wilk test. For detection of Hb-exWAGO via ELISA, optical density values from EVs and EV-depleted HES treated with and without detergent were normally distributed and were analysed using a two-way ANOVA with Šídák's correction for selected comparisons. Worm counts and faecal egg counts data were not normally distributed and were analysed using an unpaired Kruskal-Wallis test using uncorrected Dunn's test for selected comparisons. Labelled recombinant Hb-exWAGO uptake inhibition data were not normally distributed and were analysed using an unpaired Kruskal-Wallis test with Dunn's multiple comparisons test. Data analyses were performed using GraphPad Prism software version 10.1.2. Significance is denoted using asterisks where $p < 0.05$.

Author contributions

23

738 K.N., I.M.U., T.F., C.A.G. and A.H.B. designed research; K.N., I.M.U., T.F., E.R., L.S.,
739 Y.H., C.M.N., D.W., D.R.G.P., R.W., M.J.E., J.R.B.B., H.L. and C.A.G. performed
740 research; K.N., D.W., D.R.G.P., H.L., R.M.M., R.V.A., A.J.N. contributed new
741 reagents/analytic tools; K.N., I.M.U., T.F., E.R., L.S., C.M.N., D.W., J.R.B.B. and C.A.G.
742 analysed data, K.N. and A.H.B. wrote the paper.

743

Disclosure and competing interests statement

745 The authors declare that the use of exWAGO as a vaccine candidate is under the patent
746 with International Publication Number WO 2021/038250 A1.

747

Resource availability

Lead contact and material availability

750 Further information and requests for resources and reagents should be directed to and

751 will be fulfilled where possible by the lead contact, Amy Buck (a.buck@ed.ac.uk)

752

Data and code availability

754 The small RNA sequencing data are deposited to the National Center for Biotechnology

755 Information (NCBI) Sequence Read Archive (SRA) under the BioProject ID

756 PRJNA1200757. R scripts for analysis of the small RNA libraries are available at

757 https://github.com/imu93/exwago_vaccine.

758

Supplemental information

760 Document S1. Word file containing Figures S1-S4, Table S1, SI references, and legends

761 for Datasets S1 and S2.

762 Dataset S1. Excel file containing data too large to fit in a PDF

763 Dataset S2. Excel file containing data too large to fit in a PDF, related to Figure 4A

764
765
References

767
768 Andrews S (2010) FastQC: a quality control tool for high throughput sequence data.
769   *Babraham Bioinformatics*

770 Arroyo JD, Chevillet JR, Kroh EM, Ruf IK, Pritchard CC, Gibson DF, Mitchell PS,
771   Bennett CF, Pogosova-Agadjanyan EL, Stirewalt DL, *et al* (2011) Argonaute2
772   complexes carry a population of circulating microRNAs independent of vesicles in
773   human plasma. *Proceedings of the National Academy of Sciences* 108: 5003–5008

24

774 Boyaka PN (2017) Inducing Mucosal IgA: A Challenge for Vaccine Adjuvants and
775 Delivery Systems. *The Journal of Immunology* 199: 9–16

776 Britton C, Emery DL, McNeilly TN, Nisbet AJ & Stear MJ (2020) The potential for
777 vaccines against scour worms of small ruminants. *Int J Parasitol* 50: 533–553

778 Buck AH & Blaxter M (2013) Functional diversification of Argonautes in nematodes: an
779 expanding universe: *Biochem Soc Trans* 41: 881–886

780 Buck AH, Coakley G, Simbari F, McSorley HJ, Quintana JF, Le Bihan T, Kumar S,
781 Abreu-Goodger C, Lear M, Harcus Y, *et al* (2014) Exosomes secreted by nematode
782 parasites transfer small RNAs to mammalian cells and modulate innate immunity.
783 *Nat Commun* 5: 5488

784 Bukong TN, Momen-Heravi F, Kodys K, Bala S & Szabo G (2014) Exosomes from
785 Hepatitis C Infected Patients Transmit HCV Infection and Contain Replication
786 Competent Viral RNA in Complex with Ago2-miR122-HSP90. *PLoS Pathog* 10:
787 e1004424

788 Camberis M, Gros G Le & Urban J (2003) Animal Model of Nippostrongylus brasiliensis
789 and Heligmosomoides polygyrus. *Curr Protoc Immunol* 55: 19.12.1-19.12.27

790 Charlier J, Rinaldi L, Musella V, Ploeger HW, Chartier C, Vineer HR, Hinney B, von
791 Samson-Himmelstjerna G, Băcescu B, Mickiewicz M, *et al* (2020) Initial assessment
792 of the economic burden of major parasitic helminth infections to the ruminant
793 livestock industry in Europe. *Prev Vet Med* 182: 105103

794 Chow FWN, Koutsovoulos G, Ovando-Vázquez C, Neophytou K, Bermúdez-Barrientos
795 JR, Laetsch DR, Robertson E, Kumar S, Claycomb JM, Blaxter M, *et al* (2019)
796 Secretion of an Argonaute protein by a parasitic nematode and the evolution of its
797 siRNA guides. *Nucleic Acids Res* 47: 3594–3606

798 Claerebout E & Geldhof P (2020) Helminth Vaccines in Ruminants: From Development
799 to Application. *Vet Clin North Am Food Anim Pract* 36: 159–171

800 Coakley G, McCaskill JL, Borger JG, Simbari F, Robertson E, Millar M, Harcus Y,
801 McSorley HJ, Maizels RM & Buck AH (2017) Extracellular Vesicles from a Helminth
802 Parasite Suppress Macrophage Activation and Constitute an Effective Vaccine for
803 Protective Immunity. *Cell Rep* 19: 1545–1557

804 Davis MPA, van Dongen S, Abreu-Goodger C, Bartonicek N & Enright AJ (2013)
805 Kraken: A set of tools for quality control and analysis of high-throughput sequence
806 data. *Methods* 63: 41–49

807 Ding J, He G, Wu J, Yang J, Guo X, Yang X, Wang Y, Kandil OM, Kutyrev I, Ayaz M, *et*
808 *al* (2019) miRNA-seq of Echinococcus multilocularis Extracellular Vesicles and
809 Immunomodulatory Effects of miR-4989. *Front Microbiol* 10

810 Dobin A, Davis CA, Schlesinger F, Drenkow J, Zaleski C, Jha S, Batut P, Chaisson M &
811 Gingeras TR (2013) STAR: ultrafast universal RNA-seq aligner. *Bioinformatics* 29:
812 15–21

813   Ewels P, Magnusson M, Lundin S & Käller M (2016) MultiQC: summarize analysis
814   results for multiple tools and samples in a single report. *Bioinformatics* 32: 3047–
815   3048

816   Garcia-Silva MR, Cura Das Neves RF, Cabrera-Cabrera F, Sanguinetti J, Medeiros LC,
817   Robello C, Naya H, Fernandez-Calero T, Souto-Padron T, De Souza W, *et al*
818   (2013) Extracellular vesicles shed by Trypanosoma cruzi are linked to small RNA
819   pathways, life cycle regulation, and susceptibility to infection of mammalian cells.
820   *Parasitol Res* 113: 285–304

821   Geekiyanage H, Rayatpisheh S, Wohlschlegel JA, Brown R & Ambros V (2020)
822   Extracellular microRNAs in human circulation are associated with miRISC
823   complexes that are accessible to anti-AGO2 antibody and can bind target mimic
824   oligonucleotides. *Proc Natl Acad Sci U S A* 117: 24213–24223

825   Girgis NM, Gundra UM & Loke P (2013) Immune Regulation during Helminth Infections.
826   *PLoS Pathog* 9: e1003250

827   Gu W, Shirayama M, Conte D, Vasale J, Batista PJ, Claycomb JM, Moresco JJ,
828   Youngman EM, Keys J, Stoltz MJ, *et al* (2009) Distinct Argonaute-Mediated 22G-
829   RNA Pathways Direct Genome Surveillance in the C. elegans Germline. *Mol Cell*
830   36: 231–244

831   He B, Cai Q, Qiao L, Huang CY, Wang S, Miao W, Ha T, Wang Y & Jin H (2021) RNA-
832   binding proteins contribute to small RNA loading in plant extracellular vesicles. *Nat*
833   *Plants* 7: 342–352

834   Hewitson JP, Filbey KJ, Esser-von Bieren J, Camberis M, Schwartz C, Murray J,
835   Reynolds LA, Blair N, Robertson E, Harcus Y, *et al* (2015) Concerted Activity of
836   IgG1 Antibodies and IL-4/IL-25-Dependent Effector Cells Trap Helminth Larvae in
837   the Tissues following Vaccination with Defined Secreted Antigens, Providing Sterile
838   Immunity to Challenge Infection. *PLoS Pathog* 11: e1004676

839   Hewitson JP, Filbey KJ, Grainger JR, Dowle AA, Pearson M, Murray J, Harcus Y &
840   Maizels RM (2011) Heligmosomoides polygyrus Elicits a Dominant Nonprotective
841   Antibody Response Directed against Restricted Glycan and Peptide Epitopes. *The*
842   *Journal of Immunology* 187: 4764–4777

843   Hu Y, Nguyen TT, Lee ACY, Urban JF, Miller MM, Zhan B, Koch DJ, Noon JB, Abraham
844   A, Fujiwara RT, *et al* (2018) Bacillus thuringiensis Cry5B protein as a new pan-
845   hookworm cure. *Int J Parasitol Drugs Drug Resist* 8: 287–294

846   Hu Y, Zhan B, Keegan B, Yiu YY, Miller MM, Jones K & Aroian R V. (2012) Mechanistic
847   and Single-Dose In Vivo Therapeutic Studies of Cry5B Anthelmintic Action against
848   Hookworms. *PLoS Negl Trop Dis* 6: e1900

849   Jeppesen DK, Fenix AM, Franklin JL, Higginbotham JN, Zhang Q, Zimmerman LJ,
850   Liebler DC, Ping J, Liu Q, Evans R, *et al* (2019) Reassessment of Exosome
851   Composition. *Cell* 177: 428-445.e18

bioRxiv preprint doi: https://doi.org/10.1101/2025.04.01.646544; this version posted April 1, 2025. The copyright holder for this preprint (which was not certified by peer review) is the author/funder, who has granted bioRxiv a license to display the preprint in perpetuity. It is made available under aCC-BY-NC-ND 4.0 International license.

Johnson NR, Yeoh JM, Coruh C & Axtell MJ (2016) Improved placement of multi-mapping small RNAs. *G3 (Bethesda)* 6: 2103–2111

Johnston CJC, Robertson E, Harcus Y, Grainger JR, Coakley G, Smyth DJ, McSorley HJ & Maizels R (2015) Cultivation of Heligmosomoides Polygyrus: An Immunomodulatory Nematode Parasite and its Secreted Products. *Journal of Visualized Experiments* 98: e52412

Karimi ZH, Baldrich P, Rutter BD, Borniego L, Zajt KK, Meyers BC & Innes RW (2022) Arabidopsis apoplastic fluid contains sRNA- and circular RNA–protein complexes that are located outside extracellular vesicles. *Plant Cell* 34: 1863–1881

Ketting FR & Cochella L (2020) Concepts and functions of small RNA pathways in C. elegans. *Curr Top Dev Biol* 144: 45–89

King IL & Li Y (2018) Host-Parasite Interactions Promote Disease Tolerance to Intestinal Helminth Infection. *Front Immunol* 9: 2128

Lawrence RA, Gray CA, Osborne J & Maizels RM (1996) Nippostrongylus brasiliensis: cytokine responses and nematode expulsion in normal and IL-4-deficient mice. *Exp Parasitol* 84: 65–73

Li H (2023) Protein-to-genome alignment with miniprot. *Bioinformatics* 39

Liao Y, Smyth GK & Shi W (2019) The R package Rsubread is easier, faster, cheaper and better for alignment and quantification of RNA sequencing reads. *Nucleic Acids Res* 47: e47–e47

Liu J, Zhu L, Wang J, Qiu L, Chen Y, Davis RE & Cheng G (2019) Schistosoma japonicum extracellular vesicle miRNA cargo regulates host macrophage functions facilitating parasitism. *PLoS Pathog* 15: e1007817

Maizels RM (2020) Regulation of immunity and allergy by helminth parasites. *Allergy* 75: 524–534

Mantel P-Y, Hjelmqvist D, Walch M, Kharoubi-Hess S, Nilsson S, Ravel D, Ribeiro M, Grüring C, Ma S, Padmanabhan P, *et al* (2016) Infected erythrocyte-derived extracellular vesicles alter vascular function via regulatory Ago2-miRNA complexes in malaria. *Nat Commun* 7

McKenzie AJ, Hoshino D, Hong NH, Cha DJ, Franklin JL, Coffey RJ, Patton JG & Weaver AM (2016) KRAS-MEK Signaling Controls Ago2 Sorting into Exosomes. *Cell Rep* 15: 978–987

Melo SA, Sugimoto H, O'Connell JT, Kato N, Villanueva A, Vidal A, Qiu L, Vitkin E, Perelman LT, Melo CA, *et al* (2014) Cancer Exosomes Perform Cell-Independent MicroRNA Biogenesis and Promote Tumorigenesis. *Cancer Cell* 26: 707–721

Orr A, Quagraine J, Suwondo P, George S, Harrison L, Dornas F, Evans B, Caccone A, Humphries D, Wilson M, *et al* (2019) Genetic Markers of Benzimidazole Resistance among Human Hookworms (Necator americanus) in Kintampo North Municipality, Ghana. *Am J Trop Med Hyg* 100: 351–356

891   Perera DJ & Ndao M (2021) Promising Technologies in the Field of Helminth Vaccines.
892   *Front Immunol* 12: 711650

893   Prud'homme GJ, Glinka Y, Lichner Z, Yousef GM, Prud'homme GJ, Glinka Y, Lichner Z
894   & Yousef GM (2016) Neuropilin-1 is a receptor for extracellular miRNA and
895   AGO2/miRNA complexes and mediates the internalization of miRNAs that modulate
896   cell function. *Oncotarget* 7: 68057–68071

897   Qiao SA, Gao Z & Roth R (2023) A perspective on cross-kingdom RNA interference in
898   mutualistic symbioses. *New Phytologist* 240: 68–79

899   Reynolds LA, Filbey KJ & Maizels RM (2012) Immunity to the model intestinal helminth
900   parasite Heligmosomoides polygyrus. *Semin Immunopathol* 34: 829–846

901   Robinson MD, McCarthy DJ & Smyth GK (2010) edgeR: a Bioconductor package for
902   differential expression analysis of digital gene expression data. *Bioinformatics* 26:
903   139–140

904   Seroussi U, Lugowski A, Wadi L, Lao RX, Willis AR, Zhao W, Sundby AE, Charlesworth
905   AG, Reinke AW & Claycomb JM (2023) A comprehensive survey of C. elegans
906   argonaute proteins reveals organism-wide gene regulatory networks and functions.
907   *Elife* 12

908   Si F, Luo H, Yang C, Gong J, Yan B, Liu C, Song X & Cao X (2023) Mobile
909   ARGONAUTE 1d binds 22-nt miRNAs to generate phasiRNAs important for low-
910   temperature male fertility in rice. *Sci China Life Sci* 66: 197–208

911   Stael S, Miller LP, Fernandez-Fernandez AD & Van Breusegem F (2022) Detection of
912   Damage-Activated Metacaspase Activity by Western Blot in Plants. In *Plant
913   Proteases and Plant Cell Death Methods and Protocols*, Klemenčič M Stael S &
914   Huesgen PF (eds) pp 127–137. New York: Humana

915   Swarts DC, Makarova K, Wang Y, Nakanishi K, Ketting RF, Koonin E V., Patel DJ & Van
916   Der Oost J (2014) The evolutionary journey of Argonaute proteins. *Nat Struct Mol
917   Biol* 21: 743–753

918   Thompson J, Brett C, Neuhaus I & Thompson R (2022) DGEobj.utils: Differential Gene
919   Expression (DGE) Analysis Utility Toolkit. (https://cran.r-
920   project.org/package=DGEobj.utils) [PREPRINT]

921   Tran N, Ricafrente A, To J, Lund M, Marques TM, Gama-Carvalho M, Cwiklinski K,
922   Dalton JP & Donnelly S (2021) Fasciola hepatica hijacks host macrophage miRNA
923   machinery to modulate early innate immune responses. *Sci Rep* 11: 6712

924   Turchinovich A, Weiz L, Langheinz A & Burwinkel B (2011) Characterization of
925   extracellular circulating microRNA. *Nucleic Acids Res* 39: 7223–7233

926   Vidal K, Grosjean I, evillard JP, Gespach C & Kaiserlian D (1993) Immortalization of
927   mouse intestinal epithelial cells by the SV40-large T gene. Phenotypic and immune
928   characterization of the MODE-K cell line. *J Immunol Methods* 166: 63–73

929   Weaver AM & Patton JG (2020) Argonautes in extracellular vesicles: artifact or selected
930   cargo? *Cancer Res* 80: 379–381

931   WHO (2023) Soil-transmitted helminth infections.

932   Wit J, Dilks CM & Andersen EC (2021) Complementary Approaches with Free-living and
933   Parasitic Nematodes to Understanding Anthelmintic Resistance. *Trends Parasitol*
934   37: 240–250

935   Yigit E, Batista PJ, Bei Y, Pang KM, Chen CCG, Tolia NH, Joshua-Tor L, Mitani S,
936   Simard MJ & Mello CC (2006) Analysis of the C. elegans Argonaute Family
937   Reveals that Distinct Argonautes Act Sequentially during RNAi. *Cell* 127: 747–757

938   Zhang Q, Higginbotham JN, Jeppesen DK, Yang YP, Li W, McKinley ET, Graves-Deal
939   R, Ping J, Britain CM, Dorsett KA, *et al* (2019) Transfer of Functional Cargo in
940   Exomeres. *Cell Rep* 27: 940-954.e6

941   Zhang Q, Jeppesen DK, Higginbotham JN, Graves-Deal R, Trinh VQ, Ramirez MA,
942   Sohn Y, Neininger AC, Taneja N, McKinley ET, *et al* (2021) Supermeres are
943   functional extracellular nanoparticles replete with disease biomarkers and
944   therapeutic targets. *Nat Cell Biol* 23: 1240–1254

945
946

947 **Figures and Tables**
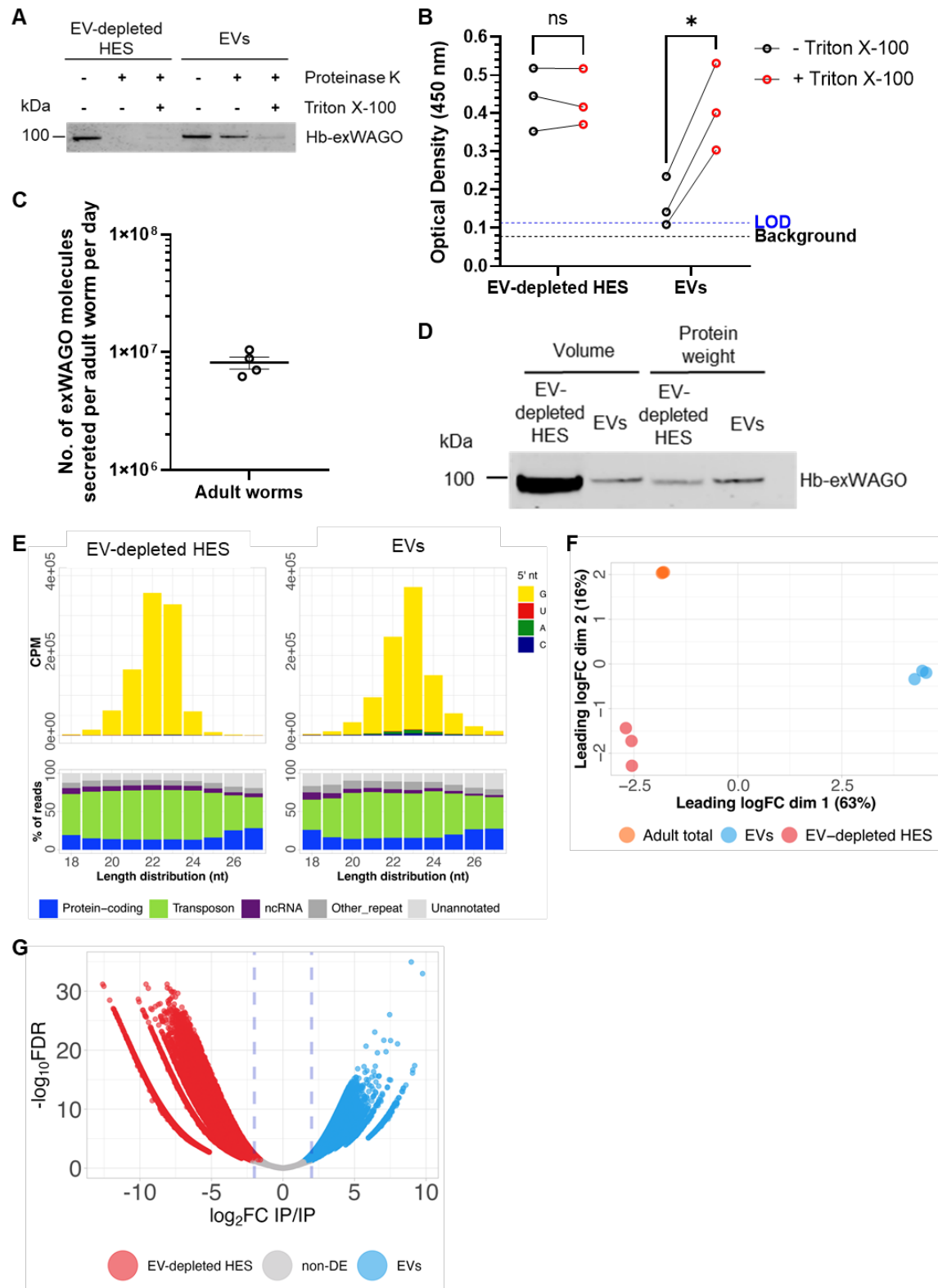
Figure 1. Hb-exWAGO is released in distinct vesicular and non-vesicular forms at high copy numbers. A) Western blot of Hb-exWAGO in EV-depleted HES or EVs following incubation in the absence or presence of Proteinase K (5 μg/ml) and/or Triton X-100 (0.05%) as indicated with 2.0 μg total protein. B) ELISA detection of Hb-exWAGO using equal protein amounts (0.2 μg) of EV-depleted HES or EVs in the presence or absence of Triton X-100 (0.05%) (n = 3 biological replicates). The limit of detection (LOD; blue dotted line) and background (no sample, black dotted line) are indicated. Significance was determined using a two-way ANOVA (ns = p > 0.05; * = p ≤ 0.05). C) Absolute copy number of Hb-exWAGO molecules present in HES, normalised per adult worm per day in culture based on sample of 30 worms (mixed sex) in culture from 24-96 hours post-harvest from mice. Data represent mean ± S.E.M (n = 4 biological replicates). D) Western blot of Hb-exWAGO in EV-depleted HES and EVs following separation by ultracentrifugation from the same volume of HES starting material (protein yield from EV-depleted HES = 38.5 μg, EVs = 2.0 μg) or using equal protein quantities (2.0 μg of each). E) Top: Length distribution and first nucleotide plots of reads mapping to the *H. bakeri* genome following Hb-exWAGO immunoprecipitation from EV-depleted HES or EVs. Data show the average length distributions (top panels) from n = 3 (CPM = counts per million). Bottom: The percentage of small RNA reads that map to different annotated regions of the *H. bakeri* genome. F) Multidimensional scaling analysis (MDS) of Hb-exWAGO small RNAs in adult worms, EVs and EV-depleted HES. Each dot represents an immunoprecipitation sample (n = 3 biological replicates), and the distance between them represents their similarity based on small RNAs aligned to distinct genomic regions. FC = fold-change. G) Volcano plot showing 45,379 genomic regions enriched in EV-depleted HES Hb-exWAGO immunoprecipitations (red) and 16,194 enriched in EVs (blue) using fold-change (FC) > 2 and false discovery rate (FDR) <0.05 as cutoffs. Non-enriched (Non-DE) regions are shown in grey. Each dot represents a distinct, non-overlapping genomic region.

976
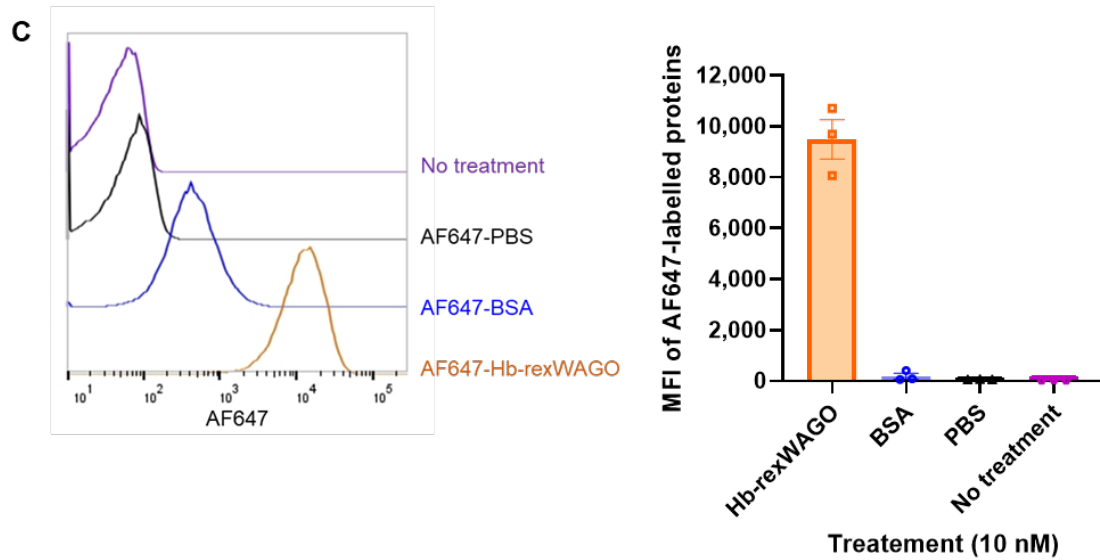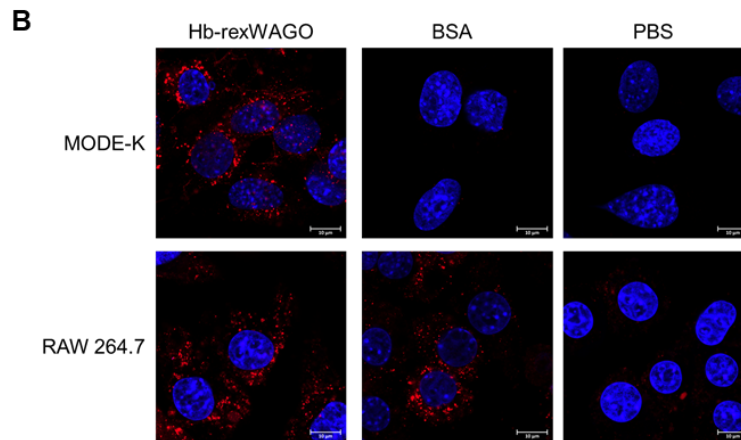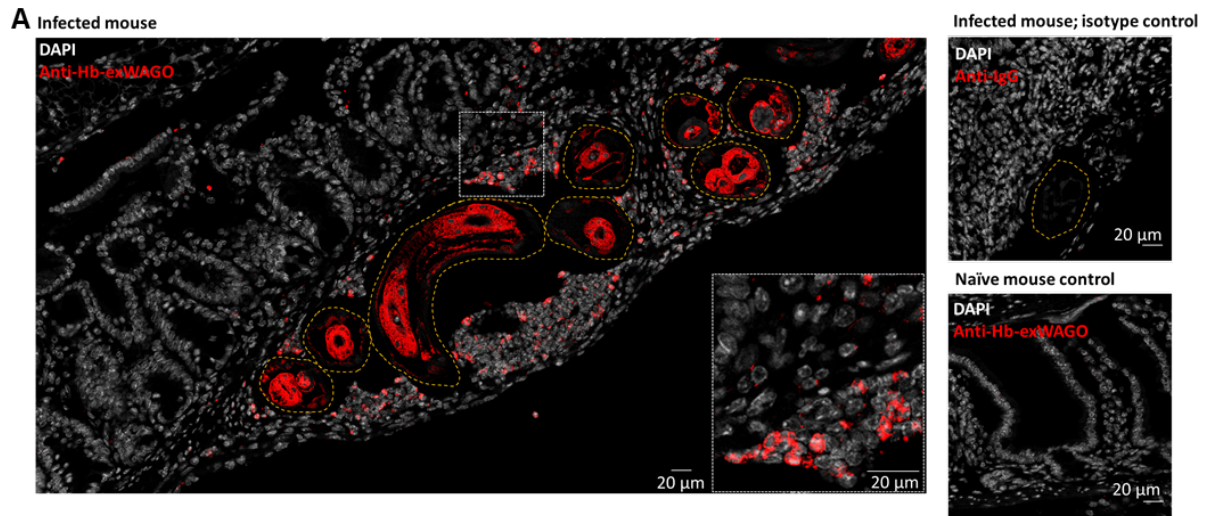
977

Figure 2. Detection of native Hb-exWAGO inside host cells *in vivo* and internalisation of recombinant Hb-exWAGO by live host cells *in vitro*. A) Confocal microscopy images of mouse gut tissue 7 days post infection with *H. bakeri* compared to uninfected gut tissue. Anti-Hb-exWAGO staining is shown in red. The outline of parasites is indicated with dotted lines. White box indicates zoomed in sections. Data are representative of 3 independent experiments. Scale bar = 20 μm. B) Confocal microscopy images of MODE-K and RAW 264.7 cells following incubation with 0.1 μM AF647-labelled recombinant Hb-exWAGO (Hb-rexWAGO), BSA or PBS for 4 hours. Scale bar = 10 μm. Data are representative of 3 independent experiments. C) The Median Fluorescence Intensity (MFI) of the AF647 signal detected by Flow cytometry analysis of MODE-K cells treated with 10 nM of AF647-labelled recombinant Hb-exWAGO (Hb-rexWAGO), BSA, PBS, or no treatment for 4 hours. Representative data are shown from 3 independent experiments (left) and data are from 3 independent experiments and show the mean ± S.E.M (right).
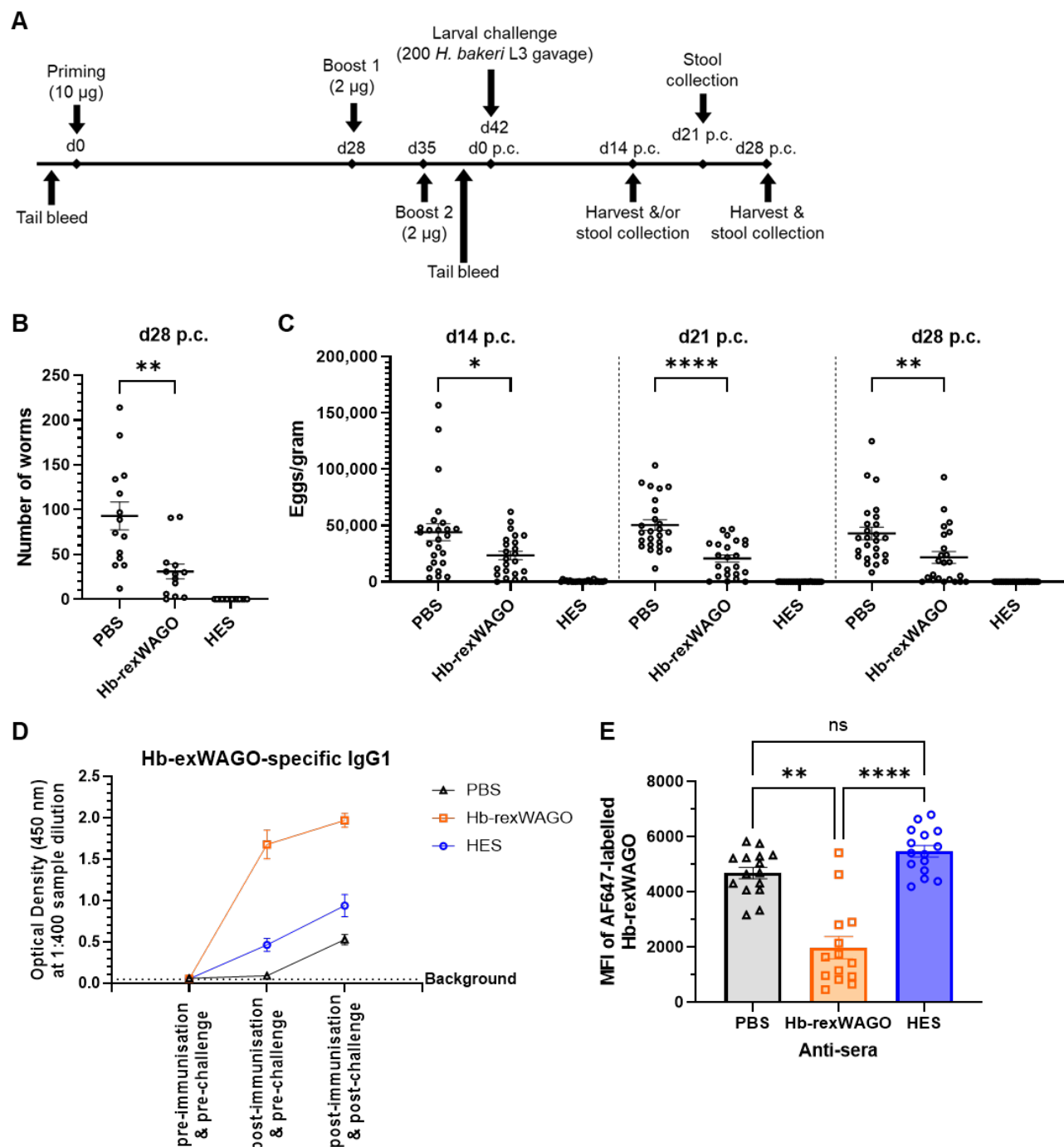
992

993

994 **Figure 3: Vaccination with Hb-exWAGO generates partial protection against**
995 **infection and generates antibodies that block Hb-exWAGO internalisation by mouse**
996 **cells.** A) Schematic of the immunisation timeline. Mice were vaccinated with recombinant

34

997   Hb-exWAGO (Hb-rexWAGO), HES, or PBS and then challenged with 200 L3 stage *H.*
998   *bakeri* larvae. B) The number of adult worms 28 days post-challenge (p.c.) recovered in
999   the small intestine following vaccination of mice and challenge with 200 L3 stage larvae
1000   (n = 14 mice per vaccination group; details in SI Materials and Methods). C) The number
1001   of eggs per gram of faeces at 14, 21 and 28 days post-challenge (p.c.). (n = 23-25 mice
1002   per vaccination group). D) ELISA detection of exWAGO-specific IgG1 antibodies in sera
1003   obtained from vaccinated mice pre-immunisation and pre-challenge (pooled serum from
1004   one experiment), post-immunisation and pre-challenge, and post-immunisation and 28
1005   days post-challenge (n = 5-14 mice per vaccination group). Data show the mean optical
1006   density at 1:400 sample dilution ± S.E.M. E) Median Fluorescence Intensity (MFI) of
1007   AF647-labelled Hb-exWAGO in MODE-K cells treated with 10 nM labelled protein for 4
1008   hours and sera (1:250 dilution) from vaccinated mice 28 days post-challenge (n = 14-15
1009   mice per vaccination group, from 3 independent experiments). All data are pooled from 3
1010   independent experiments and represent mean ± S.E.M. B, C and E) Significance was
1011   determined using an unpaired Kruskal-Wallis test (ns = p > 0.05; * = p ≤ 0.05; ** = p ≤
1012   0.01, *** = p ≤ 0.001; ****= p ≤ 0.0001).

Figure 4: ExWAGO is highly expressed in adult worms across Clade V nematodes that infect livestock and humans and binds 22-23G small RNAs. A) Expression levels of exWAGO at different developmental stages based on RNAseq data in *H. bakeri* (PRJNA750155), *N. brasiliensis* (PRJNA994163; PRJEB20824), *T. circumcincta* (PRJEB7677) and *A. ceylanicum* (PRJNA231490). Grey = no sex defined; red = female; blue = male; TPM = transcripts per million. B) ELISA detection of Hb-exWAGO in HES collected from *H. bakeri* across different life stages in the presence of Triton X-100 detergent (0.05%). Data show the mean optical density ± S.E.M (n = 2-3 biological replicates). The Limit of Detection (LOD) (dotted blue line) and background (no sample, black dotted line) are indicated. C) Western blot analysis of exWAGO from the ES of *T. circumcincta* (*Tcirc*) L4 and adults, and *T. colubriformis* (*Tcol*) adults, probed using anti-*H. bakeri*-exWAGO antibody (6.0 µg lysate loaded per sample). D) Western blot of exWAGO immunoprecipitations (IPs) using rat anti-Hb-exWAGO serum or naïve rat serum from worm lysates (WL) of *H. bakeri* (200 µg), *N. brasiliensis* (25 µg) and *A. ceylanicum* (25 µg). For each IP the volumes loaded were as follows: *H. bakeri* input (In) = 1%, unbound (UB) = 1%, eluate (IP) = 5% by volume; *N. brasiliensis* and *A. ceylanicum* In = 32%, UB = 2%, IP = 37.5%. E) Western blot of exWAGO immunoprecipitations using rat anti-Tc-exWAGO (α-Tc1 or α-Tc2) or anti-Hb-exWAGO serum from *T. circumcincta* (150 µg) worm lysate (WL). (In = 6.7%, UB = 2%, IP = 10% by volume). F) Top: length distribution and first nucleotide (nt) plots of small RNA reads mapping to each parasite genome following exWAGO immunoprecipitation, polyphosphatase treatment and small RNA sequencing from *H. bakeri*, *N. brasiliensis*, *T. circumcincta* and *A. ceylanicum* adult worms. Data show the average length distributions (*H. bakeri*: n = 3; *N. brasiliensis*: n = 2, *T. circumcincta*: n = 2, and *A. ceylanicum*: n = 2) (CPM = counts per million). Bottom: percentage of reads that map to different annotated regions of each parasite genome.